Dielectric breakdown of a random array of conducting cylinders

Mark F. Gyure and Paul D. Beale
Department of Physics, University of Colorado, Boulder, Colorado 80309
and Electromagnetic Applications, Denver, Colorado 80204
(Received 21 June 1989)

We develop a two-dimensional model for breakdown of metal-loaded dielectrics based on the breakdown of a random array of perfectly conducting cylinders embedded in a uniform dielectric and determine the breakdown field, breakdown-path geometry, and dielectric constant as a function of metal-packing fraction. The computer solution of Laplace's equation in the random geometry uses the boundary-element method and the random-packing configurations are generated by the Monte Carlo method. We compare the simulation results with exact lower bounds for the dielectric constant and scaling arguments for the breakdown field.

I. INTRODUCTION

This paper addresses the problem of dielectric breakdown in metal-loaded dielectrics, which are materials consisting of an inhomogeneous mixture of conducting and insulating components. One example is solid-fuel rocket propellant, which consists of a mixture of aluminum and ammonium perchlorate particles in a polymer binder. It has been observed[1] that the breakdown field of these materials is lowered significantly by the presence of the aluminum particles and is a strong function of the volume fraction of these particles. This unusually large sensitivity to breakdown is a safety concern in the handling and processing of solid rocket propellants and has been implicated in several accidents involving the ignition of these propellants under conditions where static electric fields are believed to have been present. Our objective is to understand factors relating to breakdown phenomena in these types of materials and to suggest nondestructive tests for breakdown sensitivity.

In this paper we describe a two-dimensional model for dielectric breakdown of these materials based on the solution of Laplace's equation in a medium consisting of a random array of conducting cylinders embedded in a uniform dielectric. In Sec. II we begin by describing the construction of randomly inhomogeneous systems of the type mentioned above, and by outlining the procedure for the solution of the Laplace equation for such systems. We then discuss the breakdown dynamics for this model by defining local breakdowns, global breakdown, and the breakdown field. Finally, in Sec. II, we define the effective dielectric constant for these systems, which we will show can be used as an indicator of breakdown sensitivity. In Sec. III we present some results of this model and make comparisons to previous work on the breakdown of metal-loaded dielectrics. In particular, we show an example of a sample which has undergone the breakdown process, and comment on the breakdown path and the evolution of the maximum electric field in the sample. We also study the dependence of the breakdown field E_b on the area fraction of conducting particles. Next, we examine the effective dielectric constant ϵ as a function of metal fraction for the randomly inhomogeneous systems and compare it to some analytically derived lower bounds. Finally, we identify two geometrical quantities that scale linearly with E_b over a large range of area fractions and that may allow for the straightforward determination of the effects of mixture composition in real materials. Section IV contains a brief summary of our results and points out directions for further study.

Breakdown phenomena in metal-loaded dielectrics have received some attention in recent years from the standpoint of percolation theory. Theoretical efforts have concentrated on lattice models in an attempt to see if the basic physical mechanisms of breakdown in these materials can be identified. Some efforts have focused on the breakdown of fuse networks[2,3] while others have concentrated on random-resistor-type networks.[4–7] We will briefly review a few of these models which are particularly relevant to our work. The model of Beale and Duxbury[4] is a bond-percolation model in which conductors are placed on the bonds of a lattice with probability p and capacitors with probability $1-p$. The capacitors are capable of sustaining a 1-V drop, after which they fail and become conductors. A voltage is applied across network and the lattice Laplace equation is solved to determine the voltages at each node and the capacitor sustaining the largest voltage drop greater than 1 V fails. The voltage is slowly increased and capacitors are allowed to fail in the manner described above, until a conducting path forms across the system. The breakdown field is defined as the minimum external voltage required to cause complete failure of the network divided by the linear dimension of the lattice. One significant result of this model is that the breakdown field $E_b \to 0$ as $p \to p_c$, where p_c is the bond-percolation threshold. In addition, E_b scales with ξ^{-1} near p_c, where ξ is the percolation correlation length and therefore E_b scales like $(p_c - p)^{\nu}$. Finally, E_b is lower for larger lattices and scales with $1/\ln(L)$, where L is the linear system size. A model by Bowman and Stroud[5] is similar to that of Beale and Duxbury; they also showed that the breakdown field E_b scales like $(p_c - p)^{\nu}$. In addition, they calculated a parameter l which is proportional to the number of bonds that need to be broken in order to

form a conducting path across the system. They showed that this parameter $l(p)$ approaches zero as p approaches p_c, but they were unable to determine conclusively the scaling of l with p. Also, they did not address whether their parameter l actually corresponds to the minimum number of bonds which need to be broken in order to form a top-to-bottom connection across the lattice, a length usually referred to as the minimum gap. In other work Stinchcombe, *et al.*[8] have suggested that the breakdown field E_b is directly proportional to some kind of minimum-gap parameter. They showed that when properly defined, this minimum gap behaves as an order parameter in the normal percolation sense and has predictable scaling behavior. This analysis was carried out for the dilute Cayley tree with the result that the minimum gap $\bar{x} \sim (p_c - p)^{\nu}$ as $p \rightarrow p_c$. Adding this to the argument of Beale and Duxbury described above, it can be concluded indirectly that $E_b \sim \bar{x}$. In Sec. III we will explore the suggestion that there may be geometrical parameters that scale simply with the breakdown field.

Our objective is to extend this lattice work to more realistic geometries by considering an approximation to arbitrarily shaped metallic inclusions randomly distributed within a perfect, lossless dielectric. In such a system the volume fraction of metal ϕ is analogous to the bond probability p, and the random close-packing limit ϕ_c replaces the percolation threshold p_c. The analogy should not be taken too far, however, since particles randomly packed into a dielectric do not have the same geometrical properties near the close-packing limit as bonds do in the lattice-percolation problem. For this reason we expect to see departures from the scaling behavior of lattice-percolation models and will explore these departures.

II. MODEL

As a starting point for a continuum model, we approximate arbitrarily shaped metallic inclusions as perfectly conducting cylinders of radius a surrounded by oxide layers $0.01a$ in thickness. We choose cylinders to keep the problem effectively two dimensional and thus more tractable from a computational standpoint. Also, we will draw analogies between this random continuous-geometry model and the two-dimensional percolationlike lattice models reviewed in the preceding section. We have included oxide layers as a practical matter since most metallic surfaces on small particles have thin oxide coatings unless carefully prepared. We will assume that the dielectric properties of the oxide are the same as those of the background dielectric, so that the effect of the oxide layers in this model is primarily to prevent any cylinder pair from initially making electrical contact.

We now focus on the construction of a model "sample." To begin with, we will assume that the background dielectric is lossless (zero conductivity) with dielectric constant unity for any applied field up to its breakdown strength. For a given area fraction ϕ of conductor the total area of the sample is fixed once the number of cylinders and their radii has been chosen; we choose a square box for the boundary of each sample. The cylinders are placed in the box randomly via the Monte Carlo method subject to the constraints that no two cylinders including their oxide layers overlap and no surface comes within two oxide layers of the boundary of the box. The result is a square two-dimensional sample consisting of perfectly conducting cylindrical inclusions occupying an area fraction ϕ of the total sample randomly distributed within a lossless dielectric.

We have chosen to apply a voltage to the sample via capacitor plates which are in contact with the top and bottom of the sample. Specifically, we place the sample between two perfectly conducting plates and extend the length of the plates to twice the sample length in order to reduce fringing fields at the edges of the sample. The result is that application of a voltage V_0 equal to the sample length produces a nearly uniform E field normalized to 1 everywhere in the sample region in the limit of $\phi \rightarrow 0$. The capacitor-plate method of applying a voltage has the advantage of providing two surfaces which define in a natural way the point at which the sample has broken down completely, i.e., a top-to-bottom connection. In addition, this configuration is consistent with experimental setups that are used and is also consistent with the way in which voltage is applied in lattice models. A final advantage to this method is that it enables calculation of an effective dielectric constant in a straightforward manner, as will be discussed later in this section.

We now turn to the matter of finding the electrostatic potential throughout a given sample, which will be used to identify regions of large electric field. Since this model assumes that all bodies are perfect conductors and that the dielectric has zero conductivity, this implies that all charge resides on surfaces or boundaries assuming all fields and charge distributions are static. This is exploited by the so-called boundary-element method,[9] which we will use to obtain an approximate solution for the charge density on all surfaces and, more importantly, the electrostatic potential of each conductor. In two dimensions, the integral solution of Laplace's equation accounting for surface charges only is

$$\Phi(\mathbf{r}) = -\sum_{j=1}^{M} \int_{C_j} \sigma(\mathbf{r}') \ln(|\mathbf{r}-\mathbf{r}'|) dl' , \tag{1}$$

where σ is the line charge density (surface charge density in three dimensions), M is the number of conductors, and Φ is the usual electrostatic potential. The boundary-element method essentially discretizes these integrals by assuming that the charge density along a line segment of sufficiently small length is approximately constant and can be replaced by a discrete charge located at the center of that line segment. If we now choose each discretized point as a place to evaluate Φ, the result is a matrix equation for the unknown charges and potentials which can be solved uniquely, provided we include M constraint equations. These equations express the fact that the net charge on any initially uncharged perfect conductor must remain zero, provided its potential is not externally specified. External voltage is coupled in through the plates, which cannot individually have zero net charge, but whose total charge can be set to zero through the addition of one final constraint equation and a corresponding unknown voltage that merely shifts the zero-voltage

reference point. The potential must be modified for points which lie on top of each other or are closer than some arbitrarily small distance for which the charges cannot be assumed to interact through the usual logarithmic potential; we choose this distance to be half a line-segment length. The self-interaction term can be found by integrating the logarithmic potential over the length of a line segment; we approximate the potential at all distances up to the cutoff by linear interpolation between the logarithmic form at a distance of half a line segment and the self-interaction at zero distance. Using this method, the unknown charges and voltages of each cylinder can be found and, hence, the electrostatic potential uniquely determined at all points in the sample.

Next, we describe how we incorporate breakdown dynamics into this model. The first step is to identify regions of the sample which are vulnerable to breakdown due to the presence of large E fields. The largest electric fields in the sample lie along lines joining the centers of cylinders which are closely spaced and whose center-to-center lines are nearly parallel to the applied field. Since the voltages are known from the boundary-element solution and we know that the largest electric fields are along these center to center lines, we approximate the E field between a pair of cylinders (or cylinders and plates) by the voltage difference between the two conductors divided by their minimum surface to surface separation distance, d. This method provides a good estimate of the average E field in the region between two conductors in the sense that this average electric field is the line integral of the actual E field along the line of minimum surface-to-surface separation divided by the length of that line. This approximation gets closer to the actual maximum local E field as d gets smaller, since the E field is being averaged over a shorter distance. We assume that breakdown occurs only between the pair of conductors which has the largest E field between them, as defined above. We then define a local breakdown as the formation of an electrical connection between two conductors resulting in those two conductors sharing charge and attaining the same electrical potential. Experimentally, it has been conjectured[1] that such local breakdowns do, in fact, occur and the presumed physical mechanism is a vaporization of a portion of the metallic particles followed by resolidification as a single conductor. We assume that the connection is a thin metallic surface between the conductors which has negligible charge density, so that the net result computationally is merely to change the constraint equations of the matrix. With these new constraints now in place, the system of equations is resolved to determine a new set of charges and voltages. Using the same criterion for breakdown, we continue this sequence of local breakdowns, storing the maximum field enhancement $E_{\max}$ which caused the local breakdown at each configuration. The sample is broken down completely when a top-to-bottom conducting connection is made. This conducting path would then rapidly discharge the capacitor plates; this is not included in our model. The minimum $E_{\max}$ in the sequence is the largest field enhancement that would be needed to break down the entire sample just as in lattice models. Hence we define the breakdown field E_b as the inverse of this minimum $E_{\max}$; as such, it is dimensionless field that is normalized with respect to the breakdown field of the background dielectric.

Finally, we want to define an effective dielectric constant for our samples and look for the behavior of ϵ as a function of area fraction ϕ. The effective dielectric constant for a medium can be defined as the dielectric constant that an isotropic, homogeneous sample of the same size and shape would need to have in order for it to have the same measured capacitance as the original inhomogeneous sample. Computationally, this amounts to replacing our samples with homogeneous samples of the same size and determining the dielectric constant they must have to induce the same total charge on the top (or bottom) plate as the original samples did. To facilitate finding ϵ, we generated a table of capacitance as a function of effective dielectric constant for our geometry using standard finite-element electrostatic codes. Knowing the capacitance for a given sample, we can now simply read the effective dielectric constant off of this calibration curve.

III. RESULTS

We now turn to a discussion of some results of this model, beginning with a few comments on some of the computational aspects. Samples containing 25 cylindrical inclusions were generated as described in the preceding section with area fractions ranging from 0.25 to 0.75; the random close-packing limit is ~ 0.81 for randomly placed impenetrable cylinders.[10] Our limit is lower (~ 0.767) due to the presence of oxide layers and the fact that our samples are not truly randomly close packed at large area fractions. This is due to an inherent difficulty in generating randomly disordered samples at large ϕ. At area fractions greater than or equal to 0.70, there is a first-order phase transition in the Monte Carlo hard-disk model from a liquid phase to a solid phase,[11] which tends to lock in our random configurations very close to the starting configuration of a square lattice. The small size of our samples, combined with the hard-wall boundary conditions, makes this problem even more acute. Consequently, for samples with $\phi \geq 0.70$, our configurations consist of fluctuations about the equilibrium solid-phase configuration, which is a square lattice for these sample sizes and boundary conditions. These configurations are statistically independent, but highly ordered. Below $\phi = 0.70$ the equilibrium phase is liquid so that random configurations are much easier to generate. Ten samples were generated at each area fraction and were run until complete failure. The results were averaged over these ten runs and the error bars on the plots in the following figures represent the standard deviation about those averages. By comparison with exact results for two cylinders in a uniform external field, we found the electric field predicted by using 16 line segments per cylinder to be within 15% of the exact result for a surface-to-surface separation distance d of $0.10a$ and $\sim 50\%$ for $d = 0.02a$, the closest allowed spacing. Despite this large inaccuracy, test cases with twice this number of patches yielded iden-

tical breakdown paths and the same breakdown field to within a few percent. The reason for this is that E_b is determined from the minimum of the maximum field enhancements; consequently, the critical local breakdown (the one that determines the breakdown field) is never between the most closely spaced pair of conductors in the system, but rather between a pair which is characterized by an intermediate or large separation relative to the average particle separation at a given area fraction. The result is that even though electric fields between some conductors are substantially in error, the overall breakdown field is considerably more accurate. Later in this section we will present results of the dielectric constant of a square lattice of cylinders as obtained from our approximate solution and compare them to analytically derived results. The generally good agreement will provide further evidence that our numerical solution is reasonably accurate. Using the above criterion of 16 discrete charges per cylinder and a lower-upper (LU) decomposition algorithm for the matrix inversion, ten runs took approximately 20 h of time on a VAX 11-780.

Figure 1 shows equipotential lines for a typical sample at an area fraction ϕ of 0.40 as a demonstration of the boundary-element solution. Notice that the capacitor plates extend far enough that the field is relatively uniform outside the sample until fringing effects take over.

Figure 2 is a representation of a typical sample with $\phi=0.45$ after complete failure. The lines between the particles indicate that a connection has been made between those particles. The numbers next to each line indicate at what point in the breakdown sequence that connection was made. One important thing to notice is the existence of connections between particles that are not part of the eventual breakdown path and the existence of other connections which represent dead ends on the main breakdown sequence. Furthermore, the breakdown path does not proceed along the shortest top-to-bottom distance, but instead winds its way through the sample. In fact, we will demonstrate that the breakdown paths tend to follow paths that pass through the smallest amount of dielectric in going from the top plate to the bottom plate. This is the continuum extension of the minimum-gap concept mentioned earlier in the context of lattice models; in this case the "gap" is the distance the path travels through the dielectric. This will be discussed in detail later in this section when we discuss the scaling properties of the breakdown field. Figure 3 indicates the value of the field enhancement which caused the breakdown of

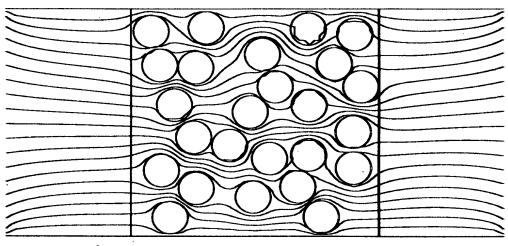

FIG. 1. Equipotentials for a typical sample with an area fraction $\phi=0.40$.

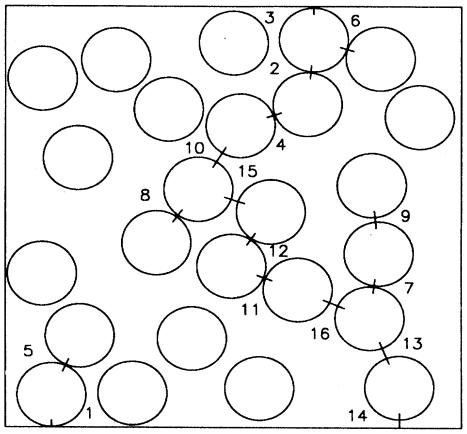

FIG. 2. Breakdown sequence illustrated for a sample with $\phi=0.45$.

each pair in the sequence. Note that the field enhancement does not increase monotonically and consequently the value of $E_{\max}$ responsible for determining the overall breakdown field (the minimum $E_{\max}$) is not the initial $E_{\max}$ in the virgin sample. The initial $E_{\max}$ does not scale with the minimum $E_{\max}$ in a simple way since the initial breakdown often is not on the eventual breakdown path. Figure 2 provides an example of this; the first breakdown is between a cylinder and the bottom plate and is part of an isolated path. This local breakdown and others like it do not increase the field enhancement in other parts of the system significantly and therefore can be more or less independent of the dynamics along the actual breakdown path.

Figure 4 shows a plot of the breakdown field E_b as a

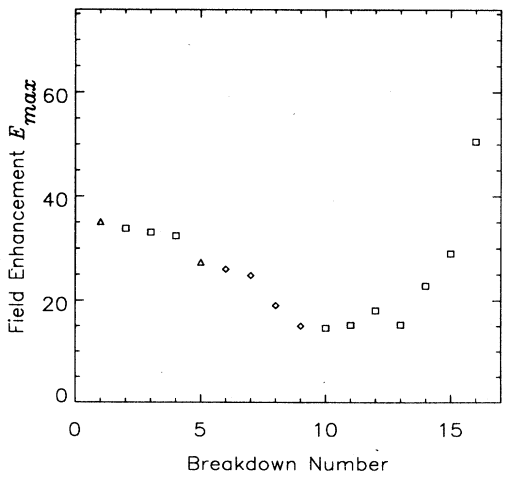

FIG. 3. Evolution of the maximum field enhancement $E_{\max}$ for the breakdown sequence shown in Fig. 2. The squares represent connections that were on the final breakdown path, the diamonds represent dead-end connections, and the triangles represent isolated connections. All quantities plotted in this and subsequent figures are dimensionless.

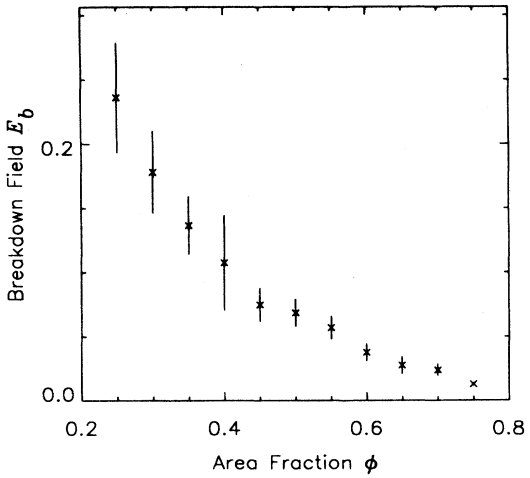

FIG. 4. Average breakdown field E_b for the random array.

function of area fraction ϕ. The breakdown field decreases monotonically with increasing area fraction as expected and E_b approaches a small but finite value as the random close-packing limit ϕ_c is approached. The breakdown field cannot go to zero because the oxide layers prevent contact between the cylinders. We will show later that this lower limit is 0.01. These results are analogous to the results obtained in lattice models where E_b decreases with increasing bond concentration p, and $E_b \to 0$ as $p \to p_c$.

Figure 5 displays a plot of effective dielectric constant ϵ as a function of ϕ for our model. The dielectric constant increases monotonically with increasing area fraction; this is easily explained physically by noting that the polarization of each sample clearly increases with increasing metal fraction. In addition, ϵ diverges as $\phi \to \phi_c$. Analogous behavior has been observed in lattice percolation where $\epsilon \to \infty$ as $p \to p_c$.[12] This effect has been measured experimentally in systems of silver particles randomly embedded in a KCl matrix.[13] In this material, special care was taken to avoid the formation of oxide layers on the silver particles; because of this; electrical contact could be made between particles, whereas in our model such contact is prevented in the virgin sample. Nevertheless, the observed behavior is qualitatively similar and the only effect is that the dielectric constant in our model cannot go to infinity at random close packing, but insteaad approaches a large but finite value. Figure 5 also shows two analytically derived lower bounds that can be placed on ϵ for any isotropic two-phase material; no upper bound exists if one phase is perfectly conducting. The Hashin bound is the best possible lower bound for a statistically isotropic two-phase material given only volume- or area-fraction information[14] and for our case where the cylinders are perfectly conducting reduces to the well known Clausius-Mossotti or Maxwell relation,

$$\epsilon = \frac{1+\phi}{1-\phi} . \tag{2}$$

The fourth-order Milton bound includes information on the statistical distribution of phases and thus is a tighter bound, but it contains some approximations that start to break down as ϕ_c is approached.[10,15] Our data as shown in Fig. 5 are consistent with the bounds described above. An additional check on the validity of our effective dielectric constant was done by considering a square array of cylinders. McPhedran[16] has derived an analytic solution for the dielectric constant of an infinite square array of cylinders embedded in a uniform external field which is valid for close spacings. We can only approximate this with our model, but a finite square array placed in between our capacitor plates should provide a reasonable test of the accuracy of our solution. Figure 6 shows the dielectric constant for our model plotted as a function of area fraction. Also shown is the approximate solution given by McPhedran in the range where it should be valid, as well as the result for the random array

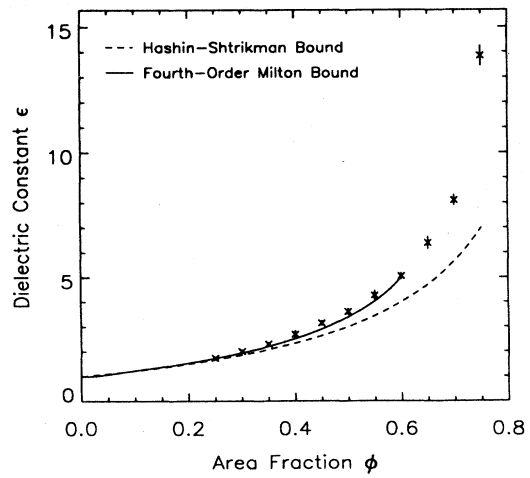

FIG. 5. Average effective dielectric constant ϵ for the random array; the crosses represent our data.

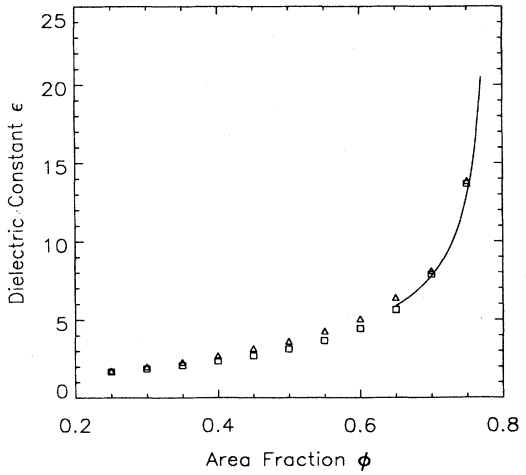

FIG. 6. Average effective dielectric constant for the square and random arrays. The squares represent the square-array data and the triangles represent the random array. The solid line is the McPhedran solution plotted over the range where it is valid.

of cylinders. The agreement between our results for the square lattice and the analytic result is quite good and can be taken as further evidence that our numerical solution for the capacitance is accurate. Finally, the McPhedran solution predicts that the dielectric constant for the ordered array should diverge like the inverse of the square root of the separation distance between cylinders. This separation distance is the minimum distance between surfaces just as we defined earlier and is calculated along a line joining cylinder centers. This separation distance is a function only of the area fraction for a fixed cylinder radius; hence, for a given area fraction and a cylinder radius of 1, we can calculate the separation distance between cylinders in the infinite square array. We find that this inverse square-root singularity also exists in our model.

Earlier we indicated the desire to find geometrical quantities that scale with the breakdown field E_b. The first candidate is the minimum gap, which was defined in the context of this model earlier in this section. The breakdown path shown in Fig. 2 certainly suggests that the backbone of the breakdown path may, in fact, be a minimum-gap path. We have calculated the minimum-gap paths for all our samples using the method of simulated annealing,[17] which has successfully solved the"traveling-salesman" problem as well as other problems of combinatorial optimization involving large discrete sets of variables. The minimum-gap problem is analogous to the "traveling-salesman" problem with the exception that we do not know how many points the minimum-gap path actually connects. This is a minor complication, however, and solution of the minimum-gap problem using the simulated annealing algorithm is quite straightforward. In addition, we have calculated the actual gap traversed in each of our samples using the quasistatic breakdown model we have described. We found that the breakdown path coincides with the minimum-gap path in over 60% of the cases, and in the vast majority of remaining cases the lengths of the actual paths are within a few percent of the minimum gap. In these cases, it is common that the actual path is some small variation from the minimum-gap path and the two paths share many of the same connections. When averaged over the ten random samples, the average actual gap is within 7% of the minimum gap in the worst case and is within about 1% in most cases. Figure 7 shows a plot of the average actual gap normalized with respect to the length of the sample as a function of area fraction ϕ. The gap decreases monotonically as the area fraction approaches the close-packing limit for our model. Figure 8 shows a plot of the breakdown field E_b as a function of the normalized minimum gap $\bar{x}$. Note that E_b scales linearly with $\bar{x}$ over nearly the entire range of data. This result confirms speculation that the breakdown field scales linearly with the minimum gap, at least for this breakdown model.

The second parameter we will consider is the average surface-to-surface separation distance of nearest-neighbor cylinders, $\bar{d}$, which we normalize with respect to the cylinder radius a. Since each local breakdown takes place between conductors which are in some sense neighbors (although not necessarily nearest neighbors), we expect that E_b may scale with this length. This quantity is much more easily calculated than the minimum gap; in fact, $\bar{d}$ is derivable from the pair correlation function $g(r)$ which is utilized in the theory of simple liquids. This correlation function $g(r)$ is well known for hard spheres in three dimensions (3D) from Monte Carlo simuations as well as analytically using the Percus-Yevick approximation.[18–22] The correlation function is also known approximately for the hard-disk problem in two dimensions (2D).[23] Once $g(r)$ is known, the probability that the first-nearest neighbor of a given particle lies a distance r away is given by

$$P(r)=2\pi nrg(r)\exp\left[-2\pi n\int_0^r dr'r'g(r')\right] \tag{3}$$

in two dimensions, and

$$P(r)=4\pi nr^2g(r)\exp\left[-4\pi n\int_0^r dr'r'^2g(r')\right] \tag{4}$$

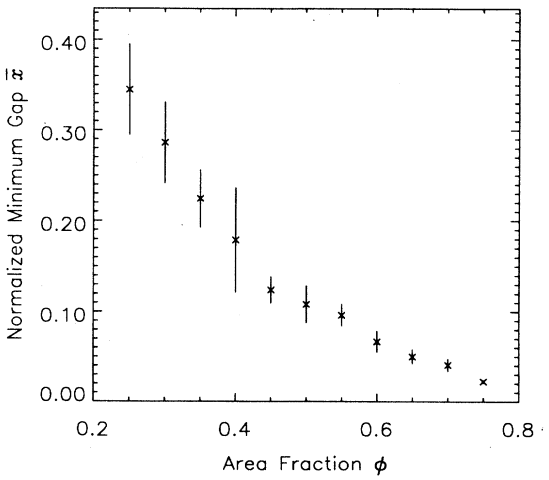

FIG. 7. Average normalized minimum gap $\bar{x}$.

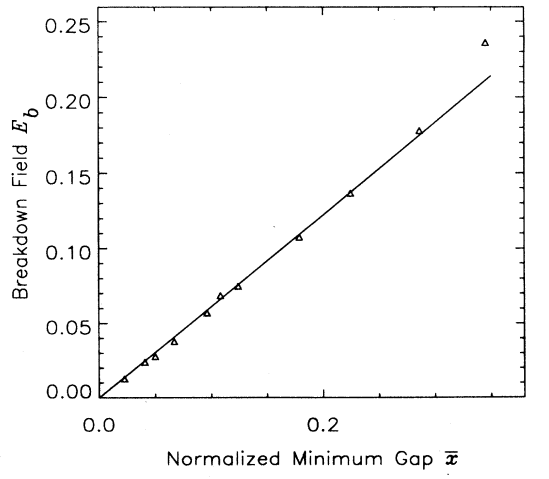

FIG. 8. Scaling of the breakdown field with the average normalized minimum gap.

in three dimensions, where n is the number density of particles. The average nearest-neighbor separation distance is then found easily by integrating the above distribution function. The result is

$$\bar{d}=\frac{1}{a}\int_0^\infty dr\, P(r)-2\ , \tag{5}$$

where $\bar{d}$ is normalized with respect to the particle radius, and the subtraction of 2 indicates that $\bar{d}$ is measured between particle surfaces rather than between particle centers. We do not calculate $g(r)$ for the hard-disk problem, although, in principle, $\bar{d}$ could be found in this manner; instead, we make a direct calculation of $\bar{d}$ from our Monte Carlo systems. Figure 9 shows a plot of $\bar{d}$ as a function of area fraction ϕ. Note that $\bar{d}$ decreases monotonically as ϕ increases as it should. Furthermore, $\bar{d}\to 0.02$ as $\phi\to\phi_c$ due to the presence of the oxide layers. Figure 10 shows a plot of E_b as a function of $\bar{d}$. Notice that E_b also scales linearly with $\bar{d}$ with a slope of $\frac{1}{2}$. The slope of $\frac{1}{2}$ can be predicted at large area fractions (small $\bar{d}$) by considering an infinite square lattice of cylinders and calculating the breakdown field in the same way we have described. In this case the average electric field across each gap is the same and E_b is determined from the first breakdown; each subsequent breakdown occurs at a larger local field. A simple calculation then shows that E_b is given exactly by

$$E_b=\frac{\bar{d}}{\bar{d}+2}\ , \tag{6}$$

where E_b is normalized with respect to the breakdown field of the dielectric and $\bar{d}$ is normalized with respect to the cylinder radius a. For small separations, the expression simply reduces to

$$E_b=\tfrac{1}{2}\bar{d}\ , \tag{7}$$

and this slope fits over the entire range of average separations for the random array. Note that since our random array is very close to a square array at area fractions near ϕ_c, this formula predicts that the breakdown field approaches 0.01 as $\phi\to\phi_c$. This lower bound is consistent with the data shown in Fig. 4.

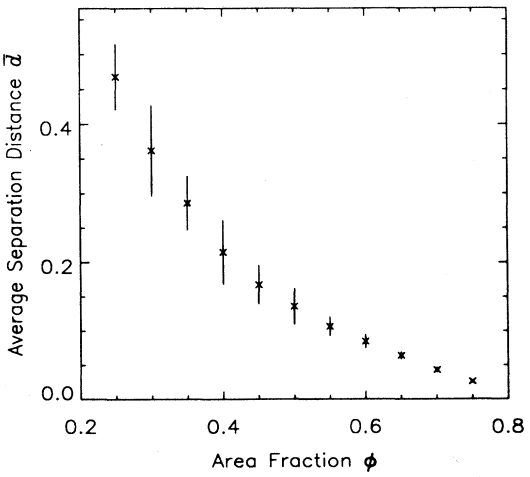

FIG. 9. Average nearest-neighbor surface-to-surface separation distance $\bar{d}$.

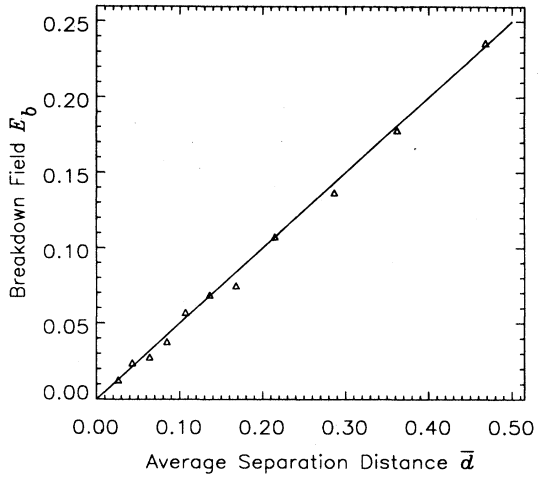

FIG. 10. Scaling of the breakdown field with the average nearest-neighbor separation distance. The line shown has slope of $\frac{1}{2}$.

IV. CONCLUSIONS

To summarize, we have introduced a new model for dielectic breakdown in random metal-loaded dielectrics which incorporates continuous-geometry effects and is hence a more realistic model than lattice models which have been focused on up to this point. In many instances, our results have confirmed results found in previous models, and in a few cases new insights have been gained. More specifically, our model predicts that the breakdown field E_b goes to 0.01 as the metal fraction ϕ approaches the close-packing limit for this model and the effective dielectric constant ϵ approaches a large but finite value; the dielectric constant cannot diverge due to the finite minimum separation between particles imposed by the presence of the oxide layers. In addition, ϵ agrees well with analytically derived lower bounds and its divergence near the random close-packing limit suggests that this could be used as a criterion for breakdown sensitivity. These results are qualitatively in agreement with the aforementioned lattice results. We have identified two geometrical parameters: the normalized minimum gap $\bar{x}$ and the average nearest-neighbor separation distance $\bar{d}$, which scale linearly with the breakdown field over nearly the entire range of area fractions studied. These results should allow for the estimation of the effects of mixture composition in a straightforward way. The average nearest-neighbor separation $\bar{d}$ can be estimated from either Monte Carlo results or by use of the pair correlation function for hard disks; similarly, the minimum gap is a parameter which is easily obtained for this model by use of the simulated annealing method, and seems to include the essential features of the original breakdown problem.

Suggestions for further study include replacing the

boundary-element method with a new approximation scheme which will allow us to analyze much larger systems than are now possible in an attempt to see system-size effects; this work is already in progress. The method being used in this new work involves multipole expansions of the scalar potential and enables us to utilize sparse matrix techniques. We were limited to 25 cylinders in this project because use of the boundary-element method results in a nonsparse matrix in which the number of unknowns goes up as the square of the total number of discrete points in the system. Hence, computing resources become strained even for modest system sizes. Using this new technique, we expect to extend this work to three dimensions and analyze systems of perfectly conducting spherical inclusions. Also, we expect to include a distribution of particle radii in both the two- and three-dimensional models. Finally, if the linear scaling of the breakdown field with the normalized minimum gap and the average nearest-neighbor separation distance can be confirmed for larger systems and for higher dimensions, the possibility exists for analyzing the entire dielectric-breakdown problem from a purely geometrical standpoint, which is computationally easier than treating the full electrostatic problem.

ACKNOWLEDGMENTS

The authors wish to thank the U.S. Army Research Office (Contract No. DAAL03-87-C-0021, Project No. P-24927-EG-S) for supporting this work. In addition, we would like to thank Ron Larson and Jim Lindsay of Electromagnetic Applications, Inc. (EMA) for their suggestions, and Vivek Sunderraj of EMA for his help in generating the effective-dielectric-constant calibration curve.

[1]R. Kent and R. Rat, J. Electrostat. **17**, 299 (1985).
[2]L. deArchangelis, S. Redner, and H. J. Herrmann, J. Phys. (Paris) Lett. **46**, L585 (1985).
[3]P. M. Duxbury, P. D. Beale, and P. L. Leath, Phys. Rev. Lett. **57**, 1052 (1986).
[4]P. D. Beale and P. M. Duxbury, Phys. Rev. B **37**, 2785 (1988).
[5]D. R. Bowman and D. Stroud, Phys. Rev. B **40**, 4641 (1989).
[6]Y. Gefen, W. H. Shih, R. B. Laibowitz, and J. M. Viggiano, Phys. Rev. Lett. **57**, 3097 (1986).
[7]H. Takayusu, Phys. Rev. Lett. **54**, 1099 (1985).
[8]R. B. Stinchcombe, R. M. Duxbury, and P. Shukla, J. Phys. A **19**, 3903 (1986).
[9]R. F. Harrington, *Field Computation by Moment Methods* (MacMillan, New York, 1968).
[10]S. Torquato and F. Lado, Proc. R. Soc. London, Ser. A **417**, 59 (1988).
[11]B. J. Alder and T. E. Wainwright, Phys. Rev. **127**, 359 (1962).
[12]J. P. Straley, Phys. Rev. B **15**, 5733 (1977).
[13]D. M. Grannan, D. C. Garland, and D. B. Tanner, Phys. Rev. Lett. **46**, 375 (1981).
[14]Z. Hashin and S. Shtrikman, J. Appl. Phys. **33**, 3125 (1962).
[15]G. W. Milton, J. Appl. Phys. **52**, 5294 (1981).
[16]G. W. McPhedran, Proc. R. Soc. London, Ser. A **408**, 31 (1986).
[17]S. Kirkpatrick, Science **220**, 671 (1983).
[18]M. S. Wertheim, Phys. Rev. Lett. **10**, 321 (1963).
[19]M. S. Wertheim, J. Math. Phys. **5**, 649 (1964).
[20]E. Thiele, J. Chem. Phys. **39**, 474 (1963).
[21]S. A. Rice and P. Gray, *The Statistical Mechanics of Simple Liquids* (Wiley, New York, 1965).
[22]J. P. Hansen and I. R. McDonald, *Theory of Simple Liquids* (Academic, London, 1986).
[23]F. Lado, J. Chem. Phys. **49**, 3092 (1968).